

Polymer-confinement-induced nematic transition of microemulsion droplets

K. NAKAYA¹, M. IMAI¹, S. KOMURA², T. KAWAKATSU³ and N. URAKAMI⁴

¹ *Department of Physics, Ochanomizu University
2-1-1, Otsuka, Bunkyo-ku, Tokyo, 112-8610, Japan*

² *Department of Chemistry, Tokyo Metropolitan University
1-1 Minami-Osawa, Hachioji-shi, Tokyo, 192-0397, Japan*

³ *Department of Physics, Tohoku University
Aoba, Aoba-ku, Sendai, 980-8578, Japan*

⁴ *Department of Physics, Yamaguchi University
1667-1 Yoshida, Yamaguchi-shi, Yamaguchi, 753-8512, Japan*

received 19 April 2005; accepted in final form 1 June 2005

published online 13 July 2005

PACS. 82.70.Uv – Surfactants, micellar solutions, vesicles, lamellae, amphiphilic systems (hydrophilic and hydrophobic interactions).

PACS. 36.20.Ey – Conformation (statistics and dynamics).

PACS. 64.70.Nd – Structural transitions in nanoscale materials.

Abstract. – We study a shape change of spherical microemulsion droplets when water-soluble polymers are confined inside of them. Upon confinement, spherical droplets deform to prolate ellipsoid droplets while keeping the total surface area and the total enclosed volume of all the droplets constant. We found that an increase of the degree of polymer confinement causes an increase in the uniaxial anisotropy of the prolate droplet, which leads to an isotropic-nematic transition in the concentrated droplet region. As a possible origin of this structural transition, we consider a loss of the conformational entropy of polymer chains due to the confinement.

Nowadays complex systems consisting of various soft materials, such as polymers, colloidal particles, liquid crystals and amphiphilic membranes, have acquired great interest because these complex materials are widely observed in biological systems and are extensively used in pharmaceutical, cosmetic, food, and other chemical industries. By doping guest soft materials to a host soft material, the dominant interactions that stabilize the structure of the host soft material are modified by additional interactions originated from the restriction of translational degrees of freedom of the guests, which brings characteristic structural transitions. The most familiar entropic interaction is the depletion interaction [1–3], which is an attractive interaction between the host soft materials caused by the reduction of the free volume of the guests. Another interesting entropic interaction is expected for confined polymer systems. For example, when polymer chains are confined between lamellar membrane slits, the membranes exhibit a phase separation between concentrated and swollen lamellae [4, 5]. In this phenomenon, the restriction of conformational entropy of polymer chains plays a crucial role.

The effects of the polymer confinement become more pronounced when polymer chains are confined inside of a spherically closed membrane. Such confinement reduces the conformational entropy of polymer chains considerably, which may induce new membrane morphologies. Lal *et al.* [6] and Javierre *et al.* [7] have investigated the structural change of the microemulsion droplets (water/SDS/alcohol/oil system) containing a polymer (polyethylene oxide: PEO) using a small-angle neutron scattering (SANS) technique. Both groups found that by confining the PEO chains inside the droplets, the size and shape polydispersity of droplets increased. We also confirmed their results using other confined polymer systems [8]. In these systems the degree of polymer confinement is not so high and if a polymer is confined in a sphere more tightly, a drastic morphology transition of enclosing membrane is expected. In this study we show a series of morphology transitions of microemulsion droplets induced by changing the degree of polymer confinement.

Since in microemulsion systems the oil and water regions are separated by surfactant monolayers, the microemulsion droplets can confine the polymer chains inside of the closed nano-space by selecting the solubility of the polymer to the solvent. As a typical example, we studied a water-in-oil microemulsion droplet system consisting of water, isooctane, surfactant AOT (sodium bis (2-ethylhexyl) sulfosuccinate), to which system a gelatin is added as a water-soluble polymer. A gelatin is a linear random-coil molecule and has high solubility to the nano-scale water pool. The gelatin is purchased from Sigma Co. Ltd. It has Bloom strength of 300 and the z -averaged molecular weight of 96000 with a rather large polydispersity [9]. The interaction between gelatin and AOT monolayers was examined by putting gelatin chains between AOT lamellar membranes in water. There was no significant change in the scattering profiles from the lamellar structure by the addition of gelatin, indicating that the adsorption or anchoring of gelatin to the AOT monolayers is negligible.

The degree of confinement of the gelatin is characterized by two parameters, *i.e.*, the ratio of the end-to-end distance of a gelatin chain in the bulk state to the diameter of a spherical water pool $R_F/2R_s$, and the average polymer weight concentration W in the water pool. The radius of gyration of a gelatin molecule R_g obtained by SANS measurements is $R_g = 89 \text{ \AA}$, and we assumed that $R_F = \sqrt{6}R_g = 218 \text{ \AA}$ for simplicity. We controlled the radius of the water pool, R_s , with keeping the total volume fraction of droplets $\phi = \phi_{\text{sur}} + \phi_{\text{dis}}$ constant, where ϕ_{sur} and ϕ_{dis} are the volume fractions of surfactant and dispersed water phase.

The samples of microemulsion droplets containing gelatin were prepared by mixing a solution of AOT in isooctane and a solution of the gelatin in water at 60°C , and then cooled to the measurement temperature. In the SANS measurements, we employed the film contrast condition, *i.e.*, we used deuterated oil, water, hydrogenated surfactant and gelatin. SANS measurements were carried out with the SANS-U instrument of ISSP at the JAERI (Tokai) and the SWAN instrument of KENS at the KEK (Tsukuba).

We first show the change in the scattering profiles induced by the confinement of the gelatin chains in the spherical microemulsion droplets in fig. 1. This experiment was performed at a dilute solution of droplets, *i.e.* $\phi = 0.07$. The scattering profile of the microemulsion droplets without gelatin has a characteristic maximum at $q_{\text{max}} = 0.06 \text{ \AA}^{-1}$ (q is the magnitude of scattering vector) and well fitted by the following expression:

$$I(q) = nP(q)S(q), \quad (1)$$

where n is the number density of droplets, $P(q)$ is the form factor for a spherical core-shell structured particle [10], and $S(q)$ is the structure factor of the Percus-Yevick model [11]. The fitting result using this model is shown by the solid line with the values of the fitting parameters $n = 5.4 \times 10^{16}/\text{cm}^3$, the length of a surfactant molecule $\delta = 8 \text{ \AA}$, and $2R_s = 119.6 \text{ \AA}$.

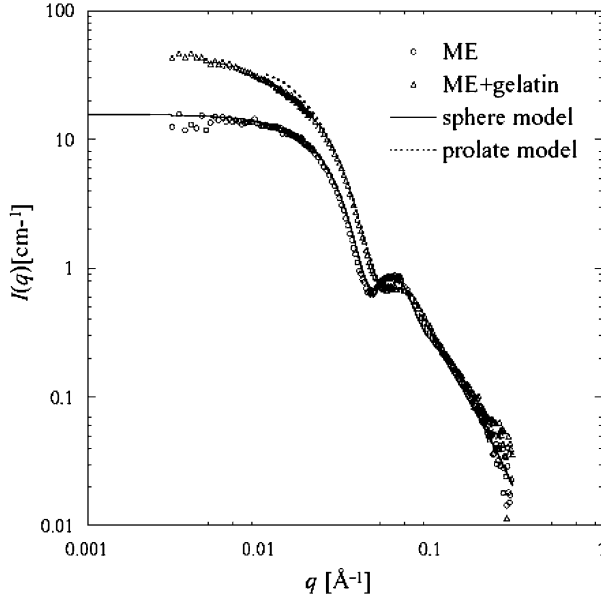


Fig. 1 – SANS profiles for water-in-oil microemulsion droplet consisting of AOT-isooctane-water at $\phi = 0.07$ without (circle) and with (triangle) gelatin of $W = 9\%$ at 30°C . The solid and dashed lines are fitting results with the sphere core shell and the prolate core shell model, respectively. The quantitative $S(q)$ of the prolate model is obtained from our Monte Carlo simulation.

By introducing the gelatin chains inside the droplets, the characteristic maximum shifted to a larger value of $q_{\text{max}} = 0.08 \text{ \AA}^{-1}$, and the scattering intensity in the low- q region increased considerably. In this case, the degree of confinement is $R_F/2R_s = 1.82$ and the gelatin concentration in the water pool is $W = 9.1 \text{ wt}\%$. In contrast to the pure droplet microemulsion, several features of the scattering profile of the microemulsion containing the gelatin cannot be explained by the scattering function of the spherical model. Instead we can fit the observed profile using a prolate core-shell model for which the following analytical expressions for the scattering function are available [12],

$$\langle P(q) \rangle = \int_0^1 |F(q, x)|^2 dx, \quad (2)$$

$$F(q, x) = (B_c - B_m) \frac{4}{3} \pi a_c R_c^3 \left[3 \frac{j(u_c)}{u_c} \right] + (B_m - B_s) \frac{4}{3} \pi a R^3 \left[3 \frac{j(u)}{u} \right], \quad (3)$$

$$u_c = q R_c \sqrt{a_c^2 x^2 + (1 - x^2)}, \quad u = q R \sqrt{a^2 x^2 + (1 - x^2)}. \quad (4)$$

Here, R and R_c are the outer and inner radii of the prolate minor axis, a and a_c are the axial ratios of the outer and inner radii, respectively, and $j(x)$ is the first-order spherical Bessel function. The scattering length densities B_c , B_m , B_s correspond to the core, the membrane, and the solvent, respectively. The above expressions reduce to those of the spherical core-shell model when $a = a_c = 1$. The structure factor $S(q)$ for the prolate model was obtained by the Monte Carlo simulation of hard spherocylinders with corresponding rod size and volume fraction. In this paper, we used the prolate ellipsoid model to fit the form factor of the scattering profiles, whereas we used the spherocylinder model to obtain the structure factor.

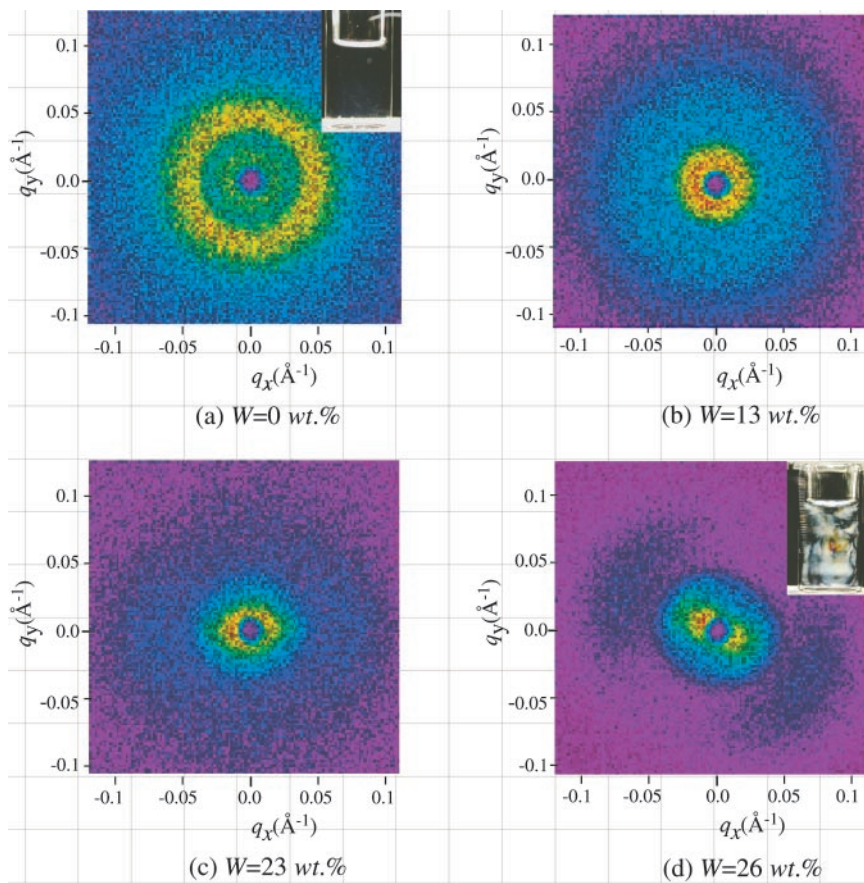


Fig. 2 – The two-dimensional SANS patterns of the microemulsion confining polymer chains at 33 °C. The volume fraction of the water pool in the microemulsion is fixed to $\phi = 0.4$. Concentrations of added polymer are (a) $W = 0$, (b) 13, (c) 23, and (d) 26 wt%. Inset figures in (a) and (d) are the corresponding crossed polarizers photographs.

This is due to the lack of the analytical expression of the form factor for the spherocylinder shape. To our knowledge the difference between the prolate ellipsoid model and the spherocylinder model does not make a significant change on the fitting results of the experimental profiles. The fitted curve using this model is given in fig. 1 by the dashed line that agrees well with the observed profile. The obtained fit parameters are $R_c = 41.3 \text{ \AA}$, the mean axis ratio $a_m = (a + a_c)/2 \sim 4$ and $n = 4.0 \times 10^{16} / \text{cm}^3$. This means that the averaged number of gelatin chains per droplet is roughly 0.8. Thus, the microemulsion droplet deforms from the spherical shape to the rod-like one by confining gelatin chains. It is known that the sphere-to-rod transition is achieved by changing the elastic parameters of membrane [13,14]. From neutron spin echo experiments, however, we confirmed that the bending rigidity of AOT microemulsion membrane is not changed by the confinement of gelatin chains [15]. Then, this result opens up a new possibility to control the membrane morphologies.

Based on the above experimental results, we expect that the rod-like droplets exhibit an isotropic-nematic transition when droplets are concentrated. Figure 2 shows the evolution of the 2D scattering patterns of a concentrated solution of droplets ($\phi = 0.4$) as a function of

the polymer concentration W at 33 °C. Here we fixed $R_F/2R_s = 1.43$. Without gelatin, the scattering pattern shows an isotropic ring arising from the characteristic form factor peak, which is pronounced by the suppression of the scattering intensity in the low- q region due to the structure factor. By the addition of gelatin up to $W = 13$ wt%, the scattering ring was shifted toward $q \sim 0.08 \text{ \AA}^{-1}$ with the decreased scattering intensity, and the scattering intensity in the low- q region is increased. This indicates that the droplets start to become a rod-like shape, which is consistent with that of the dilute droplet system (fig. 1). At this gelatin concentration, the scattering pattern was still isotropic. At $W = 23\%$, the scattering pattern begins to show a slight anisotropy and further increase of the gelatin concentration ($W = 26\%$) brings a highly oriented rod-like droplet phase. In order to support this assertion, we show the corresponding crossed polarizers photographs of concentrated ($\phi = 0.4$) microemulsion droplets without gelatin (inset of fig. 2a) and with strongly confined gelatin ($R_F/2R_s = 1.43$, $W = 26\%$; inset of fig. 2d) in a vial. Without gelatin the photo image is homogeneously dark, indicating an isotropic structure. On the other hand, the microemulsion droplets confining polymer chains show a colored and heterogeneous texture similar to the Schlieren texture of a nematic phase. These results clearly demonstrate that the isotropic-nematic transition of the rod-like droplets is induced by the gelatin confinement. The interesting point here is the fact that combining a spherical droplet and a spherical polymer coil spontaneously forms an anisotropic structure.

Here we discuss the geometrical constraints in the sphere-to-rod transition. The radius of the minor axis of the prolate droplet ($R_c = 41.3 \text{ \AA}$) was about 2/3 times smaller than the radius of the spherical droplet without gelatin ($R_s = 59.8 \text{ \AA}$). Using Helfrich's bending elastic model of a surfactant monolayer, the equilibrium shape of the droplet is determined by the following Hamiltonian [16]:

$$f_{\text{mem}} = \int [2\kappa(H - C_0)^2 + \bar{\kappa}K] dS, \quad (5)$$

where κ and $\bar{\kappa}$ are the bending and Gaussian moduli, H and K the mean and Gaussian curvatures, C_0 the spontaneous curvature, and S the surface area of the droplet. In addition to this elastic energy, we have the incompressibility condition, *i.e.*, the total surface area of all droplets and the total enclosed volume of all droplets satisfy

$$nS\delta = \phi_{\text{sur}}, \quad (6)$$

$$nV = \phi_{\text{dis}}, \quad (7)$$

respectively, where V is the volume of a droplet and n is the number density of droplets. The morphology of the microemulsion droplet is determined by an optimization of the elastic energy under the constraints of the incompressibility, eqs. (6) and (7) [14]. When the most stable shape is a sphere, its radius R_s is simply given by

$$R_s = 3\delta\phi_{\text{dis}}/\phi_{\text{sur}}, \quad (8)$$

which means that the radius is fixed so long as the droplets are spherical. Since this constraint holds very strictly, the size of a spherical droplet containing large polymer chains cannot change unless it deforms. On the other hand, the incompressibility constraint on the rod-like droplets (for simplicity, we assume a sphero-cylindrical shape) is expressed by

$$R_c = \frac{2 + 2a_{\text{sc}}}{2 + 3a_{\text{sc}}} R_s, \quad (9)$$

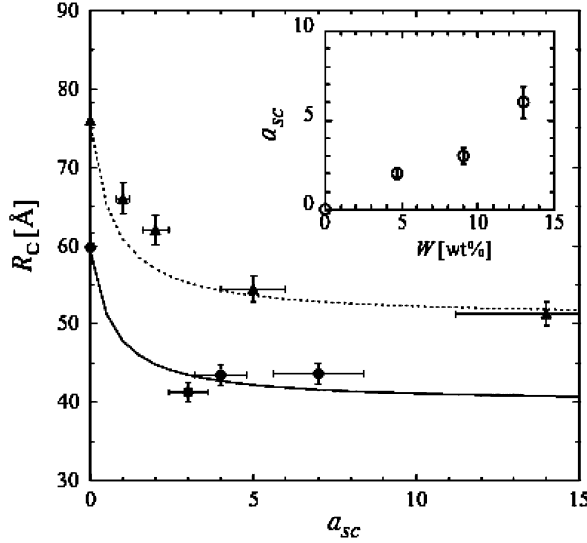


Fig. 3 – The relationship between a_{sc} and R_c for the different conditions of the polymer confinement at $\phi = 0.07$. The experimental values for $R_F/2R_s = 1.82$ (closed circle) and $R_F/2R_s = 1.43$ (closed triangle), and solid and dashed lines are calculated by eq. (9). The inset figure shows the relationship between the gelatin concentration W and a_{sc} .

where a_{sc} is the axis ratio of the sphero-cylinder, $a_{sc} = a_m - 1$. In the limit of $a_{sc} \rightarrow \infty$, we obtain $R_c = (2/3)R_s$ from eqs. (8) and (9). Here, the volume fraction of the polymer chains is included in ϕ_{dis} . It should be noted here that the number of droplets per unit volume should decrease owing to the conservation law when the transition takes place. We measured the scattering profiles of the droplets containing gelatin as a function of the gelatin concentration W for two samples with $R_F/2R_s = 1.82$ and $R_F/2R_s = 1.43$ at $\phi = 0.07$. We show in fig. 3 the relationship between a_{sc} and R_c obtained by the fitting of the scattering profiles. The inset figure shows the relationship between W and a_{sc} . With increasing W , the length of the rod-like droplets increases, which is consistent with the nematic transition induced by the gelatin confinement (fig. 2). For both samples having different $R_F/2R_s$ values, the experimentally obtained relationship between a_{sc} and R_c agrees well with eq. (9). Thus we confirmed that the size of the droplets after the transition is determined by the incompressibility condition.

Finally, we give some free-energy considerations on the microemulsion droplets containing polymer chains. The total free energy per unit volume F_{tot} of the system essentially consists of the following two terms:

$$F_{tot} = n_i(f_{mem} + f_{conf}), \quad (10)$$

where n_i ($i = s, c$) is the number density of spherical (s) and cylindrical (c) droplets. The morphology of the microemulsion droplets confining polymer chains is determined by minimizing F_{tot} . The elastic energy per droplet f_{mem} is given by eq. (5), and f_{conf} represents the polymer confinement energy per droplet. When the self-avoiding polymer chains are confined inside of either a spherical or a cylindrical space, the corresponding free energy increase is [17]

$$f_{conf} = n_p^i \alpha_i k_B T \left(\frac{R_F}{2R_i} \right)^{\frac{5}{3}}, \quad (11)$$

where n_p^i is the number of polymer chains per droplet ($i = s, c$), and α_i is an unknown

numerical constant. Since the total number of polymer chains should be conserved, we have the relation $n_p^c n_c = n_p^s n_s$. The first term in eq. (10) represents the stability of the microemulsion droplets without polymer. Since the original empty droplets prefer the spherical shape, the relation $n_s f_{\text{mem}}^s < n_c f_{\text{mem}}^c$ holds for the given experimental conditions. Consequently, the dominant driving force for the transition should be the polymer confinement energy $n_i f_{\text{conf}}^i$. From the relation $R_c = (2/3)R_s$ and the above-mentioned conservation law $n_p^c n_c = n_p^s n_s$, the necessary (but not sufficient) condition for the shape transition to occur is that the numerical coefficients in eq. (11) satisfy $\alpha_c/\alpha_s \leq (2/3)^{5/3}$. Unfortunately, we cannot compare the numerical values of α_c and α_s , because eq. (11) is obtained only within the scaling argument. This issue will be discussed in our forthcoming paper [15].

In conclusion, by confining polymer chains inside of the microemulsion droplet, the membrane morphology changes from the spherical shape to the rod-like one, and further increase in the degree of polymer confinement brings the isotropic-to-nematic transition in the concentrated droplet region. We also confirmed that the constraint of the incompressibility is well satisfied in the morphological transition, and that the necessary condition for this transition is that the numerical coefficients in eq. (11) satisfy $\alpha_c/\alpha_s \leq (2/3)^{5/3}$.

* * *

The SANS experiments were done under the approval of Neutron Scattering Program Advisory Committee of ISSP and KENS. This work was supported by Grant-in-Aid for Exploratory Research (No. 15740261) from the Ministry of Education, Sciences, and Culture of Japan.

REFERENCES

- [1] ASAKURA S. and OOSAWA F., *J. Chem. Phys.*, **22** (1954) 1255.
- [2] ANDERSON V. J. and LEKKERKERKER H. N. W., *Nature*, **416** (2002) 811.
- [3] ADAMS M., DOGIC Z., KEKKER S. L. and FRADEN S., *Nature*, **393** (1998) 349.
- [4] DAOUD M. and DE GENNES P. G., *J. Phys. (Paris)*, **38** (1977) 85.
- [5] LIGOURE C., BOUGLET G. and PORTE G., *Phys. Rev. Lett.*, **71** (1993) 3600.
- [6] LAL J. and AUVRAY L., *J. Phys. II*, **4** (1994) 2119.
- [7] JAVIERRE I., BELLOCQ A. M. and NALLET F., *Langmuir*, **17** (2001) 5417.
- [8] NAKAYA K. and IMAI M., *J. Phys. Soc. Jpn. Suppl. A*, **70** (2001) 338.
- [9] PEZRON I., DJABOUROV M. and LEBLOND J., *Polymer*, **32** (1991) 3201.
- [10] GUINIER A. and FOURNET G., *Small-Angle Scattering of X-rays* (Wiley, New York) 1995.
- [11] PERCUS J. K. and YEVIC G. J., *Phys. Rev.*, **110** (1958) 1.
- [12] KOTLARCHYK M. and CHEN S.-H., *J. Chem. Phys.*, **79** (1983) 2461.
- [13] SVERGUN D. I., KONAREV P. V., VOLKOV V. V., KOCH M. H. J., SAGER W. F. C., SMEETS J. and BLOKHUIS E. M., *J. Chem. Phys.*, **113** (2000) 1651.
- [14] SAFRAN S. A., *Statistical Thermodynamics of Surfaces, Interfaces, and Membranes* (Addison-Wesley Publishing Company) 1994.
- [15] NAKAYA K., IMAI M., KOMURA S., KAWAKATSU T. and URAKAMI N., in preparation.
- [16] HELFRICH W., *Z. Naturforsch.*, **28c** (1973) 693.
- [17] DE GENNES P. G., *Scaling Concepts in Polymer Physics* (Cornell University Press) 1979.